Available online at www.sciencedirect.com
ScienceDirect
Journal of Molecular Graphics and Modelling 25 (2006) 304–312
Journal of Molecular Graphics and Modelling
www.elsevier.com/locate/JMGM

Modelling NifH2 protein of *Clostridium pasteurianum* reveals clues about its physiological function

Murat Kasap *

Kocaeli University, Department of Medical Biology, Faculty of Medicine, 41380 Umuttepe, Kocaeli, Turkey

Received 28 April 2005; received in revised form 19 January 2006; accepted 19 January 2006
Available online 21 February 2006

Abstract

Clostridium pasteurianum is an anaerobic free-living nitrogen fixer. As a unique feature, the organism contains five extra *nifH*-like genes in addition to *nifH1*. Detailed analysis with respect to the structure and function of the *nifH*-like gene products is missing due to the lack of information about the presence of their translation products in the cell. Recent work indicates that the *nifH2* gene is transcribed and translated into a polypeptide of expected size in nitrogen-fixing cells of *C. pasteurianum* and is regulated both at the transcriptional and translational levels. However, the current data do not reveal the physiological function of the NifH2 protein. In this study, we have used computer tools and the NifH1 of *C. pasteurianum* as the template to predict a possible tertiary structure and assign a putative function for NifH2 protein. A comparison of the structures of the NifH1 and modelled NifH2 revealed similarities in the polypeptide conformations for both monomers. Analysis of the properties of nucleotide binding, dimer interacting and cluster containing regions did not reveal major differences between NifH1 and modelled NifH2, although minor differences were observed. Rigid docking results revealed the possibility of formation of a NifH1–NifH2 heterodimer as well as formation of a NifH2 homodimer. We, therefore, propose that NifH2 can form a dimer with NifH1, albeit less efficiently and may function as a regulatory Fe-protein.

Keywords: Nitrogen fixation; NifH2; Computer modelling

1. Introduction

Biological nitrogen fixation is catalyzed by the enzyme nitrogenase. With one exception [1], all known nitrogenases are complexes of two metalloproteins. Although some organisms contain more than one type of nitrogenase [2], the extensively characterized conventional nitrogenase is a molybdenum-containing enzyme and consists of the MoFe protein and the Fe protein. The MoFe protein is an $\alpha_2\beta_2$ tetramer, which contains two types of metal centers, the FeMo-cofactor and the P-cluster [3]. The iron protein is a homodimer and contains four Fe atoms organized into a single Fe_4S_4 cluster [4]. All nitrogenase activities require the presence of both components, and the N_2 reduction site which is believed to be located on the MoFe protein [5]. In some cases, purified MoFe protein from one bacterial species reconstitutes an enzymatically active hybrid nitrogenase with the purified Fe protein of other species [6,7].

Clostridium pasteurianum is a gram positive, anaerobic, free-living nitrogen-fixing bacterium. This species has an historical importance in nitrogen-fixation research because it was the first free-living nitrogen-fixing organism isolated, and the first consistent cell-free nitrogen fixation was demonstrated with this organism [8]. Extensive nitrogen fixation studies have been performed with *C. pasteurianum*. Information relevant to the regulation of nitrogen fixation [9,10], identification of the structural genes of nitrogenase component proteins (Fe- and MoFe-proteins) [11], solution of the X-ray crystal structure of MoFe protein [3,12], the sequences of the *nif* and *nif*-associated genes, their organization and putative functions [13] has been obtained. The regulation of nitrogenase synthesis and nitrogen-fixing activity in *C. pasteurianum* in batch and continuous cultures was studied previously [14,9,15,10] and recently [16]. No nitrogen-fixing activity was found in cultures growing on excess ammonia [9,16]. When a fixed nitrogen source is added to a nitrogen-fixing culture of *C. pasteurianum*, the synthesis of nitrogenase abruptly stopped after ammonia addition for at least several doublings [9,16].

* Tel.: +90 2623591230; fax: +90 2623037003.
E-mail address: mkasap@vt.edu.

1093-3263/$ – see front matter © 2006 Elsevier Inc. All rights reserved.
doi:10.1016/j.jmgm.2006.01.006

The sequences of nitrogen fixation genes of *C. pasteurianum* were determined [17]. Several distinct features were recognized including an overlap between *nifD* and *nifK* and the fusion of *nifN* and *nifB* into *nifNB*. Besides these interesting features, the presence of extra *nifH* homologues was reported in *C. pasteurianum* (*nifH2* through *nifH6*). Among them *nifH1* encodes the subunits of the well known Fe protein. A key function of the Fe protein is the integration of nucleotide binding and MgATP hydrolysis with electron transfer between its Fe_4:S_4 cluster and the MoFe protein. A recent study revealed that *nifH2* and *nifH6* encode the same polypeptide that can be found under nitrogen-fixing conditions and expressed in parallel to the well known NifH1 protein [18]. This observation creates a need to revisit the studies on regulation of nitrogen fixation in *C. pasteurianum*, because co-presence of a second NifH1-like protein might affect regulation of nitrogen-fixing activity.

At present, the physiological role of NifH2 protein is not known and unfortunately genetic tools that can aid manipulation of *C. pasteurianum* to develop NifH2 mutants are not yet well developed [18]. In this study, we attempted to find clues about the role of NifH2 protein using computer modelling as the tool and the crystal structure of the NifH1 protein as the template. In overall, we examined the modelled NifH2 tertiary structure and compared it with the known NifH1 structure. Specific attention was paid to the details of dimer interface, metal cluster, nucleotide binding pocket and MoFe protein interacting residues. Our specific aim was to determine if a NifH1–NifH2 heterodimer formation is possible and if it is possible could this heterodimer be active in nucleotide hydrolysis and electron transfer to the MoFe protein.

2. Materials and methods

Since there is no three-dimensional structure determined for NifH2 protein, we built a comparative model based on NifH1 protein sequence retrieved from Swiss-Prot database (http://www.expasy.org/sprot/ under the accession number of P09552). An html form was created and contained all the information needed by Swiss-Model server (http://www.swiss-model.expasy.org). We instructed the server to use NifH1 protein of *C. pasteurianum* as the template of interest. The crystal structure for NifH1 is available in PDB entry 1CP2 [19]. The form was submitted to the Swiss-Model server via electronic mail and the result was obtained similarly in pdb format.

The quality of the resulting model was assessed by the root mean square deviation (RMSD) between equivalent atoms in the model and template structure. Beyond using RMSD to assess the quality of the model, we have used TM-score (http://bioinformatics.buffalo.edu/TM-score), which is a new scoring method reliably used in several predictions before [20].

The predicted NifH2 structure was analyzed with two different visualization programs, namely Swiss-Pdb Viewer and MolMol, both of which are freely available in the following URLs: http://www.expasy.org/spdv/ and http://hugin.ethz.ch/wuthrich/software/molmol/, respectively. In Swiss-Pdb Viewer, molecules were superimposed with iterative magic fit tool under fit menu. In MolMol, molecules were superimposed with fit tool under edit menu. In Swiss-Pdb Viewer, specific amino acid residues were selected from the control panel whenever needed. In MolMol, selection dialog box was used. The existence of hydrogen bonds was predicted with compute H-bonds tool of Swiss-Pdb Viewer. Ramachandran diagrams were examined via MolMol. Distribution of electrostatic potentials and temperature factors were calculated in MolMol. Because the charges for all residues are not normally given in PDB files, we used a standard macro (pdb-charge) to assign the proper charges to the residues and manually checked whether all charges were assigned accurately. To calculate electrostatic potential, *CalcPot* tool was used and the results were stored in a *pot* file. After the addition of contact surfaces with *AddSurface* tool, calculated potentials were read with *Readpot* tool and painted to the surfaces with the *Paint* tool. NifH1 and NifH2 amino acid sequences were aligned using ClustalW [21]. Molecular weights and isoelectric points of NifH1 and NifH2 polypeptides were calculated with a molecular biocomputing suite [22].

To predict formation of a NifH1–NifH2 complex, ClusPro, an automated docking and discriminating method for prediction of protein complexes, was used via web-based server (http://nrc.bu.edu/cluster) [23]. Docked conformations were generated using the docking program DOT based on Fast-Fourier Transform correlation approach. Default values of 1 Å grid-step and 4 Å surface-layers were used. Docked complexes were selected and ranked based on a hierarchical clustering method [24].

To define the rigid and flexible regions of NifH1 and NifH2 proteins, FIRST software was used [25]. It is freely available through http://firstweb.asu.edu/. FIRST determines floppy inclusion and rigid substructure topography of a given protein structure, based on a set of distance constraints determined by the covalent and hydrogen bonding network within a single conformation of the protein. Analysis of rigidity and flexibility is meaningless without the inclusion of explicit hydrogens. Because for NifH1 and NifH2, the hydrogen atom positions are not experimentally defined we added hydrogens with Reduce, which is a program for adding hydrogens to a Protein Data Bank (PDB) molecular structure file. Reduce uses proper PDB standard names and also optimizes the orientation of rotatable polar hydrogens. Hydrogens are added in standardized geometry with optimization of the orientations of OH, SH, NH_3^-, Met methyls, Asn and Gln sidechain amides, and His rings. Reduce is implemented in MolProbity which is an interactive macromolecular structure validation tool provided by the Richardson laboratory at Duke University at http://kinemage.biochem.duke.edu/molprobity/index-king.html.

3. Results

3.1. Model building

The tertiary structure of NifH2 protein was modelled in Swiss-Model server. Superimposition of the modelled NifH2

backbone generated a seemingly perfect fit with the NifH1 backbone as shown in Fig. 1A. Also, examination of Ramachandran plots of the backbone angles of NifH1 structure and NifH2 model showed that they both fall into commonly observed regions of phi–psi space (Fig. 1B). However, a model cannot be claimed accurate or precise unless its atomic coordinates are not within 0.5 Å RMSD of the template structure [26]. The RMSD of the C-alpha coordinates for the NifH2 model was 0.08 Å of the NifH1 template structure, which indicated a very fine model prediction. The accuracy of the generated model was further supported by calculating the TM-score [27]. The value of the TM-score for NifH2 model was 0.99 which indicated a very fine model prediction as well (for meaningful predictions, TM-score should be bigger than 0.4). The low value of root mean square deviations from ideal bond distances and angles and the high value of TM-score suggested that the modelled NifH2 structure is very similar to the template as we expected. In addition, NifH2 protein is 92% identical to the NifH1 protein at the amino acid level. The high level of amino acid sequence identity bolsters the validity of the NifH2 model. Comparison of the superimposed structures indeed revealed many structurally equivalent regions between the backbones of NifH1 template and NifH2 model (Fig. 1A).

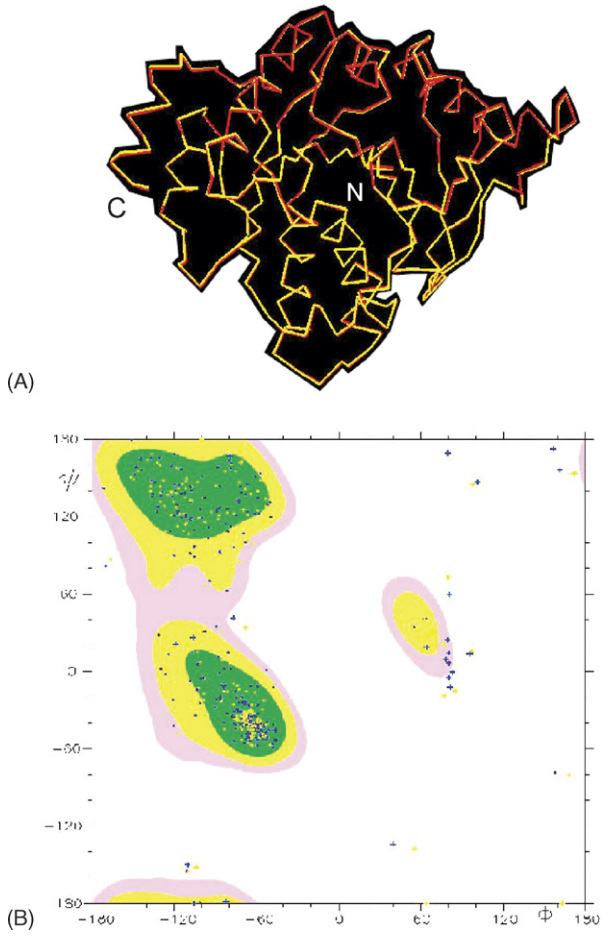

Fig. 1. (A) Superimposition of C-alpha backbones of NifH1 protein and NifH2 model. C-alpha backbone of NifH1 is shown in yellow and C-alpha backbone of NifH2 is shown in red. C is the C-terminal and N is the N-terminal end of the proteins. The figure was prepared in Swiss-Pdb Viewer. (B) Ramachandran plot for NifH1 template and NifH2 model was prepared using MolMol.

3.2. Analysis of NifH2 topology

The structure of Fe protein of nitrogenase from *C. pasteurianum* has been refined to 1.93 Å by Schlessman et al. [19]. Each subunit in the iron protein dimer (NifH1 protein) exhibits a topology of an eight-stranded β-sheet flanked by nine α-helices (Fig. 2A). We observed a similar topology in NifH2 model, having the same number of mixed helix/sheet polypeptide fold (Fig. 2B). The twisted β-sheet core of the NifH1 protein contains seven parallel and one short antiparallel β-strands. The twisted β-sheet core of the NifH2 model also contained seven parallel and one antiparallel β-strand with the same strand order. The single antiparallel strand is located at one edge of the β-sheet as it was observed in NifH1 template. Beyond overall similarities, however, there were two noticeable differences between NifH1 structure and NifH2 model that probably reflect contributions from sequence variations. First, the antiparallel β-strand in NifH2 model appeared to be a residue longer than the one observed in NifH1 template (Fig. 2C). The primary amino acid sequence comparison between NifH1 and NifH2 polypeptides after the sequence alignment within the region of 70–80 in which the short antiparallel β-sheet structure is located revealed two amino acid differences between NifH1 template and NifH2 polypeptides. Glu76 of NifH1 is replaced by Thr 76 in NifH2 and Gly78 in NifH1 is replaced by Ala78 in NifH2 (Fig. 3). The change in primary amino sequence may have dictated formation of a longer β-sheet structure in NifH2 model. Second, the helix structure formed by the residues 64–66 in NifH2 model positioned in a noticeably different angle than in the NifH1 tertiary structure (Fig. 2D). The difference in the helix region, however, is not expected to affect the physiological properties of NifH2 protein since these residues are away from any of the residues that have crucial roles in either dimer interface or nucleotide binding or MoFe protein interaction.

3.3. The Fe_4:S_4 cluster of NifH2 protein

The thiol ligands of Cys94 and Cys129 from each Fe protein subunit (NifH1 template and NifH2 model) coordinate the cubane Fe_4:S_4 cluster (Fig. 3, bolded cysteine residues). As in NifH1, the NifH2 Fe_4:S_4 cluster is supported by the main chain residues of Gly93, Ala95, Gly96, Arg97, Gly98, Asp126, Val127, Val128, Gly130, Gly131, Phe132. These invariant residues are critical for maintaining the appropriate cluster environment. Analysis of the cluster environment of NifH1 template and NifH2 model showed that the key amino acid residues involved in cluster stabilization are located at the same position and in an identical orientation (Supplement 1), which implies that Fe_4:S_4 cluster of the NifH2 protein may be capable of electron transfer to the MoFe protein, provided that the NifH2 dimer accurately interacts with the MoFe protein. However, the polarity of the other residues around the Fe_4:S_4 cluster and around the above-mentioned invariant residues has

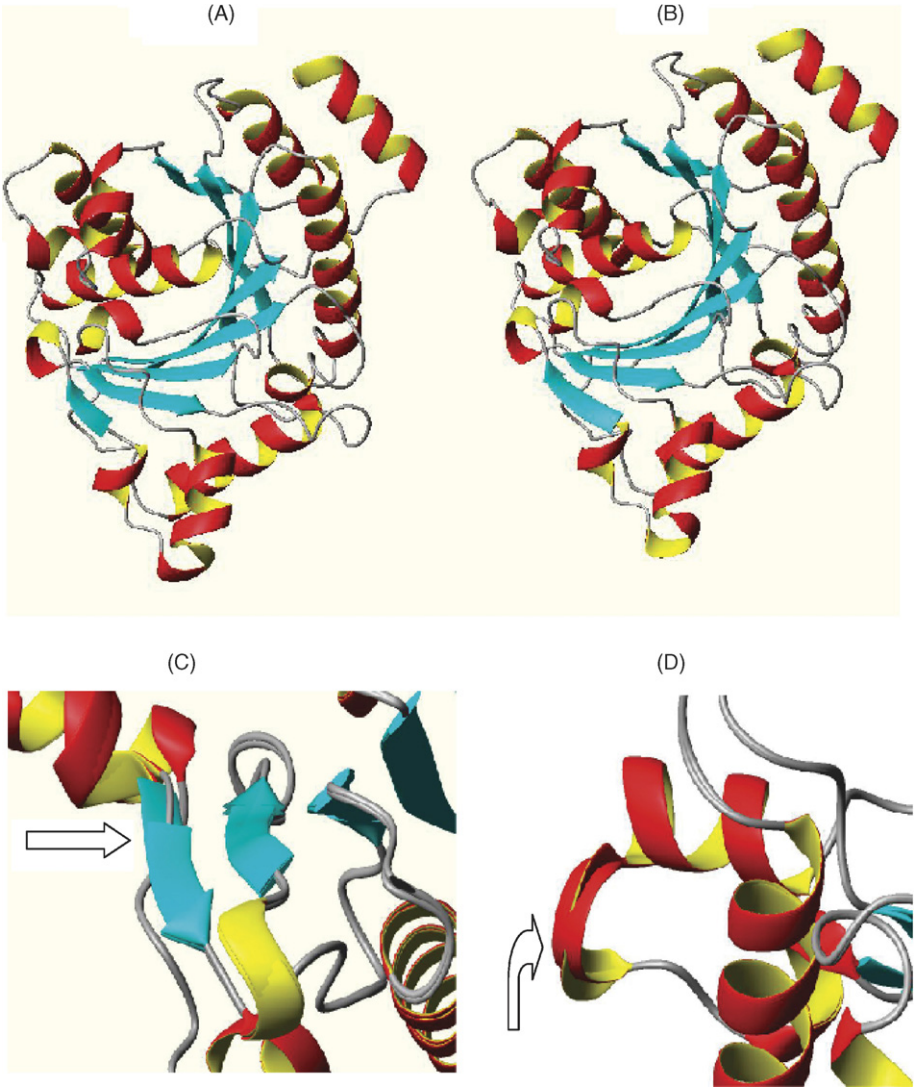

Fig. 2. (A) Ribbon diagram of NifH1 protein drawn using MolMol. (B) Ribbon diagram of NifH2 model drawn using MolMol. (C) Comparison of the short β-sheet structures after superimposition of NifH1 template on NifH2 model reveals a residue longer β-sheet formation in NifH2 model as shown with an arrow. (D) Comparison of the α-helical structures after superimposition of NifH1 template on NifH2 model reveals a different positioning of the α-helix structure formed by residues 64–66 as shown with an arrow.

to be considered before such a prediction is made, because the midpoint potential of the cluster environment is affected by the surrounding residues and thus the electron transfer process to the MoFe protein. Despite identical orientation and similar positioning of the key residues around the Fe_4:S_4 cluster, we observed differences in distribution of electrostatic surface potentials around the key residues suggesting that the efficiency of the electron transfer by NifH2 may be different than by NifH1.

3.4. Dimer interface

The Fe_4:S_4 cluster covalently bridges two NifH1 subunits forming a homodimer. NifH2 may also form a NifH2–NifH2 homodimer, as it may form a NifH1–NifH2 heterodimer. To explore both possibilities, we first looked at the dimer interface in detail, and then created rigid docking models. Schlessman et al. [19] reported 42 residues that play a direct role in dimer formation (residues indicated in Fig. 3). Analysis of the sequence alignment between NifH1 and NifH2 showed that the 42 dimer-forming residues are conserved and are located at the same position in an identical orientation in tertiary structures. We did not observe any structural difference as determined by C-alpha tracing between the NifH1–NifH1 dimer interface and the NifH1–NifH2 dimer interface indicating that both dimer compositions are likely to be formed (Supplement 2).

We further explored the possibility of NifH1–NifH2 dimer formation by building several rigid docking models via ClusPro Server using NifH1 as the receptor and NifH2 as the ligand. Candidate docked models were selected based on the known crystal structure of NifH1 homodimer. After a through examination, one of the NifH1–NifH2 heterodimer was selected as the most likely candidate and compared with the known structure of NifH1–NifH1 homodimer (Fig. 4). For near native predictions with ClusPro, the average ligand RMSD

Fig. 3. ClustalW alignment of the sequences of NifH1 and NifH2 proteins. Residues associated with binding to the MoFe protein and to nucleotide are indicated with the following symbols, respectively: (!) and (^). Residues involved in dimer interaction within Fe-protein are indicated with (#). There are 22 different residues between NifH1 and NifH2. Residues that differ between NifH1 and NifH2 are colored other than black. Thiol ligands of Cys94 and Cys129 which coordinate the cubane Fe_4:S_4 cluster was bolded in black.

is reported to be 5 Å and a model within a certain fixed cluster radius of <10 Å C-alpha RMSD is likely to be a close prediction to the native structure [23]. To calculate C-alpha RMSD for NifH1–NifH2 model, the model was moved along the *X*-axis to ensure covering of all the interaction space with NifH1 homodimer, and then RMSD was calculated. The calculated RMSD for NifH1–NifH2 portion for the over-posed structure was 6.8 Å indicating that a near native predicted model was obtained via ClusPro Server. We, therefore, can propose that NifH2 may form a heterodimer with NifH1 creating a NifH1–NifH2 iron protein. We similarly created a NifH2 homodimer via ClusPro Server and compared it with the NifH1 homodimer. The calculated RMSD for NifH2 homodimer for the overimposed structure was 5.1 Å indicating that a NifH2 homodimer is structurally more similar to NifH1 homodimer than a NifH1–NifH2 heterodimer. Kasap and Chen [18] reported formation of two dimers in a native gel, which slightly differ in their molecular weight and run slightly different locations. We expect to see formation of an active NifH1 homodimer as previous studies confirm. The docking results also imply that one of the bands observed on the native gel might contain a NifH1–NifH2 heterodimer. By examining molecular weights and p*I* values of the possible dimers (NifH1 homodimer, NifH2 homodimer, NifH1–NifH2 heterodimer) it is not possible to predict whether the second band is a NifH2 homodimer or it is a NifH1–NifH2 heterodimer or a mixture of both, because the molecular weight and p*I* values of NifH1 and NifH2 dimers are highly similar (Table 1).

3.5. *Nucleotide binding region*

MgATP binds to homodimeric Fe protein and hydrolysis of MgATP regulates the transfer of electrons from the Fe_4:S_4 cluster to the MoFe protein. At least 23 key residues play roles in nucleotide binding by NifH1 of *C. pasteurianum* ([19,28]; also indicated in Fig. 3). Analysis of the sequence alignment between NifH1 and NifH2 proteins showed that the 23 nucleotide binding residues are conserved. Some of these residues are located within the P-loop, switch I and switch II regions. Since switch I provides communication between the nucleotide and the Fe protein surface involving MoFe protein interactions [29–31], and switch II provides communication between nucleotide binding site and the Fe_4:S_4 cluster [32,33], NifH2 is expected to have similar communications. The P-loop contributes to all direct interactions of the Fe protein with the phosphates of nucleotides through hydrogen bonding [34]. When the P-loop region of NifH1 was superimposed with the P-loop of NifH2 using C-alpha atoms, the position and orientation in two structures are strikingly similar (Supplement 3). This illustrates that the interaction between the P-loop and the bound Mg^{2+} and phosphates of nucleotides is similar for these proteins. In addition, overall C-alpha tracing

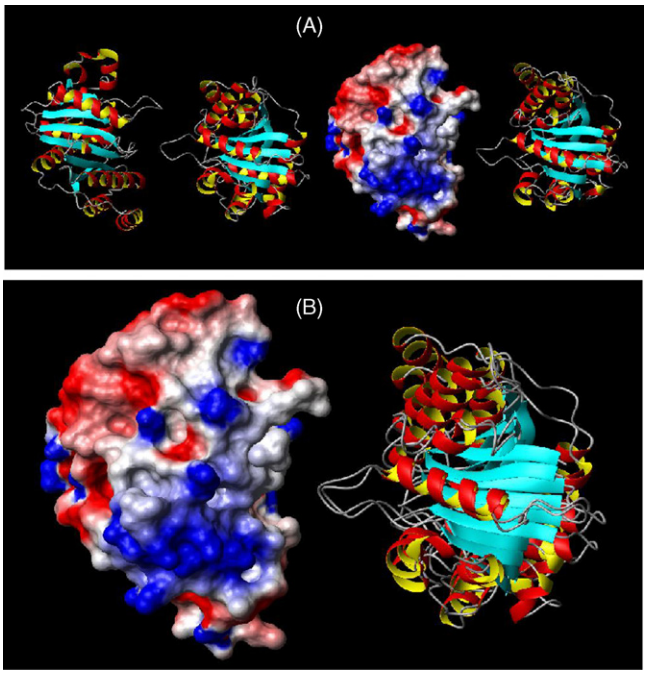

Fig. 4. Results from rigid-body docking simulations between NifH1 and NifH2 monomers. Illustrations are created in MolMol and 15 Å space was created between each monomer for the sake of easy presentation. In panel A-left part, a NifH1 homodimer is shown for the purpose of comparison. In panel A-right part, a NifH1–NifH2 heterodimer is shown. The electrostatic surface potential of the NifH1 monomer in NifH1–NifH2 heterodimer was illustrated. In panel B, NifH1–NifH2 heterodimer was moved along the *X*-axis to ensure covering all of the interaction space with NifH1 homodimer and to calculate RMSD.

of the key residues and similar distribution of the electrostatic surface potentials for the key residues in NifH1 template and NifH2 model revealed a similar nucleotide binding pocket, which strongly implies that the putative NifH2 homodimer or NifH1–NifH2 heterodimer may be capable of binding nucleotides.

3.6. MoFe protein interaction region

At least 20 key residues play roles to provide a contact between iron protein and MoFe protein ([19]; also indicated in Fig. 3). Analysis of the sequence alignment between NifH1 and NifH2 proteins showed a conservation of the 20 MoFe protein interacting residues. C-alpha tracing of the key residues in both the NifH1 template and the NifH2 model revealed a similar surface pattern (Supplement 4). Furthermore, a previously defined region (residues 59 through 67 in *Azotobacter vinelandii*, which is shown to be important in Fe protein MoFe protein interactions [35]), is conserved in both NifH1 and NifH2 proteins. Therefore, the putative NifH2 homodimer or NifH1–NifH2 heterodimer are most likely capable of interacting with the MoFe protein provided that they are able to hydrolyze ATP and go into necessary conformational changes.

Table 1
Comparison of the calculated molecular weights and isoelectric points of NifH1 and NifH2 dimers

Dimer	Molecular weight (kD)	p*I*
H1–H1	59.31	4.90
H2–H2	59.21	4.97
H1–H2	59.11	5.05

3.7. Analysis of the different residues between NifH1 and NifH2

There are 22 different residues between NifH1 and NifH2 proteins. None of these residues are within the key residues that affect dimer formation, nucleotide binding and MoFe protein interaction. Two regions appear to concentrate on possessing the different residues. Region 1, which is the region between amino acid 26 and 31, contains helix-turn-turn-bend-coil-coil motif in both proteins having a similar tertiary structure. Region 2, which is the region between amino acid 245–249, however, contains helix-helix-coil-coil-coil in NifH2 model and helix-bend-coil-coil-coil fold in NifH1 protein. In overall, both proteins display similar solvent accessible surface areas (11,686 $Å^2$ in NifH1 and 11,702 $Å^2$ in NifH2). Mapping the electrostatic potentials to the protein surfaces revealed significant amount of similarity between the two proteins indicating that in overall both proteins do have similar folding properties and stability (Fig. 5). However, closer examination of the overall surface areas revealed regions that do differ in their electrostatic properties (especially the above-mentioned regions). Observation of such regions indicates that NifH1 and NifH2 have several regions that differ in their flexibility and rigidity. This is important information especially considering that the Fe protein goes under conformational changes before interacting with MoFe protein.

3.8. Flexibility analysis

The results of FIRST analysis for NifH1 and NifH2 showed that both proteins have large virtually rigid cores along with several less rigid regions (Fig. 6). Rigid regions of both proteins do not possess the key residues that have roles in dimer formation and MoFe protein interaction. In overall, NifH2 appear to be more flexible in dimer interacting regions and less flexible in MoFe interacting regions. For instance, helix 4 and 8 of NifH2 are more flexible than helix 4 and 8 of NifH1 and these regions contain 13 of the dimer interacting residues. Yet, helix 2 and 3 of NifH2 is less flexible than helix 2 and 3 of NifH1 and these regions contain 9 of the MoFe protein interacting residues. A plausible interpretation of this observation is that although NifH2 may form a heterodimer with NifH1, the heterodimer may not interact with MoFe protein properly. This interpretation agrees with the overall analysis in that a NifH1–NifH2 heterodimer most likely creates a less active/inactive nitrogenase.

To make sure that FIRST analysis is valid, we compared NifH1 residue rigidity/flexibility results with β-factors from the *C. pasteurianum* NifH1 crystal structure. β-factors are a measure of the relative stability of a local area in a molecule. A low temperature factor (blue color) indicates relatively little movement of that particular part of the molecule, and a high

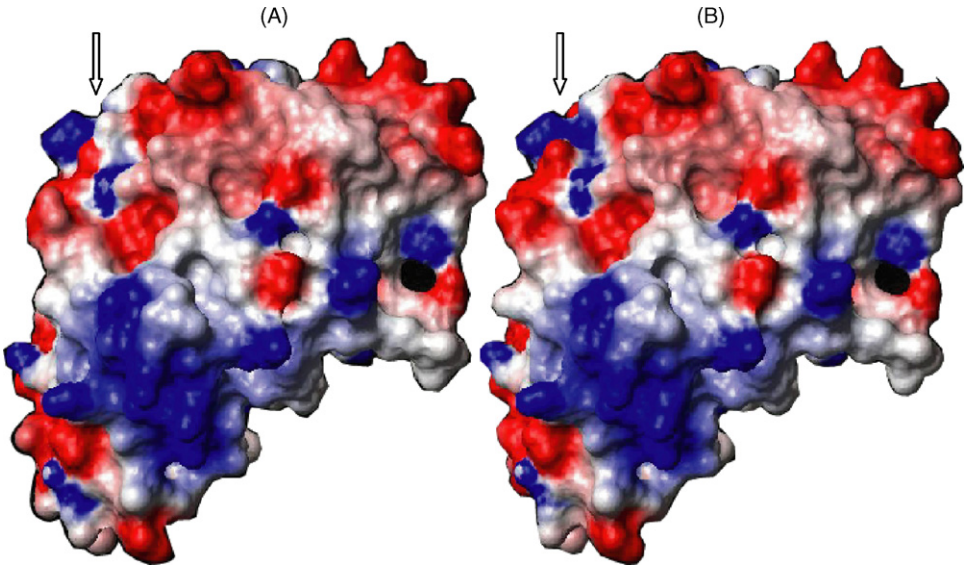

Fig. 5. Electrostatic surface potentials of NifH1 (A) and NifH2 (B). Figure is generated using MolMol, which solves Poissen–Boltzman equation and displays the electrostatic potential on the molecular surface. Arrows highlight an area differs in their electrostatic surface potentials between NifH1 and NifH2.

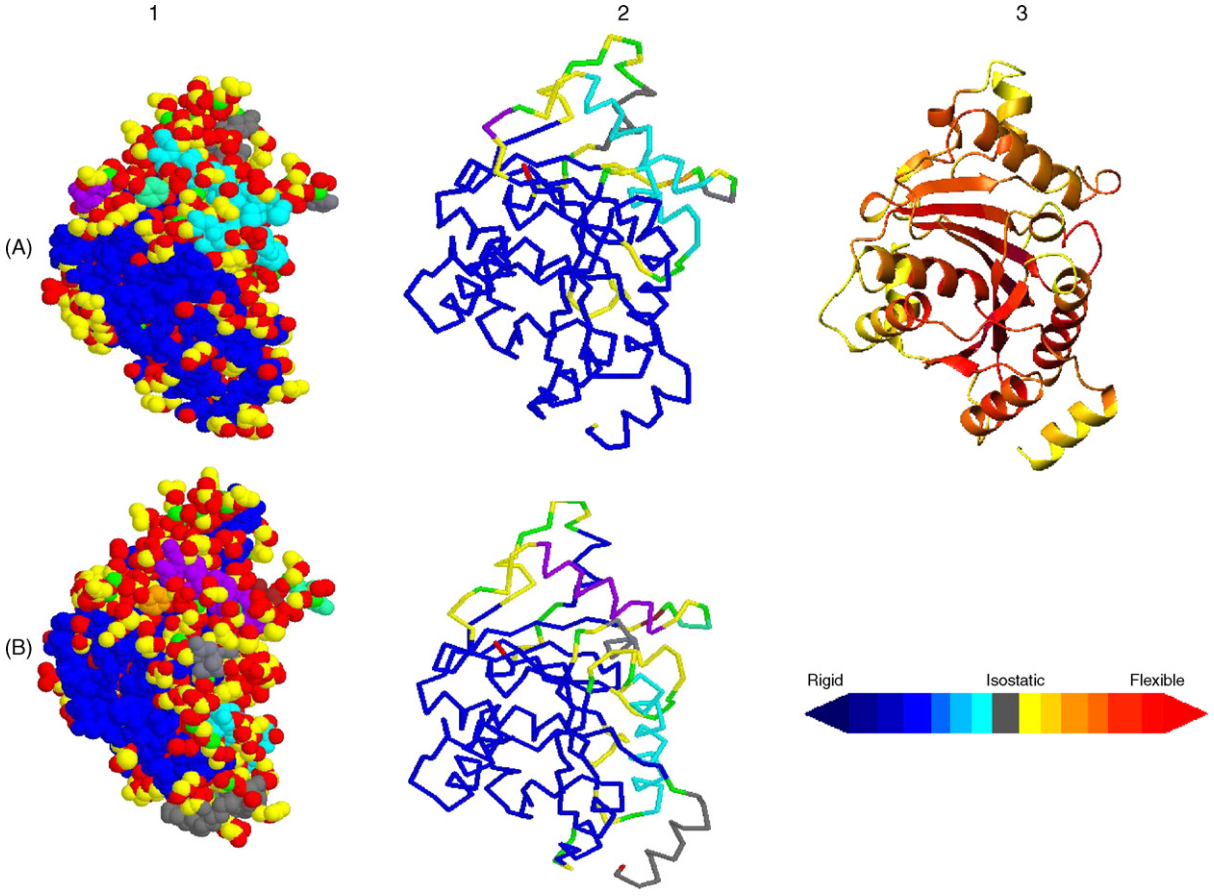

Fig. 6. Space fill and backbone diagrams of NifH1 template and NifH2 model showing the flexible and rigid regions of the NifH1 (A1–A2) and NifH2 (B1–B2) colored by flexibility index. Gray regions are isostatic. Blue regions are overconstrained, having more than enough bonds to make them rigid. Yellow to red regions are flexible. In A3, a ribbon diagram of β-factors for NifH1 crystal structure was included to compare the FIRST results with the available crystallography data.

temperature factor (red color) indicates rapidly moving sections of the molecule. Although the pdb (1cp2) structure of *C. pasteurianum* was determined under cryo-temperature, regions of higher β-factors correlated well with more flexible regions in NifH2 indicating that FIRST analysis results are reliable (Fig. 6).

4. Discussion

Structural analysis performed in this study indicates that NifH1 and NifH2 tertiary structures are similar enough to possess similar biochemical properties. The sequence comparison shows invariant residues in regions associated with cluster and nucleotide binding indicating that a NifH2 homodimer may be capable of coupling hydrolysis of ATP and electron transfer. In addition, docking results suggest possible formation of a NifH2 homodimer as well as formation of a NifH1–NifH2 heterodimer. In overall, the present view implies that *C. pasteurianum* may possess three different Fe proteins formed by NifH1 and NifH2 monomers. It is already known that the previously characterized Fe protein is a highly active NifH1 homodimer and responsible for (whole or majority of) the measured Fe-protein activity [15]. In here, we propose that the Fe protein formed by NifH2 (a NifH2 homodimer) would most likely create a less active nitrogenase since a NiH2 homodimer created by rigid docking does not superimpose well with the known tertiary structure of NifH1 homodimer. There are examples of nitrogen-fixing organisms which possess two NifH proteins. For instance, in Rhizobium ORS571, two copies of *nifH* seem to share the total nitrogen-fixing activity (NifH1 accounts for 70% and NifH2 for 30%) [36].

Rigid docking results also suggest formation of a NifH1–NifH2 heterodimer and this dimer is most likely an inactive complex since it significantly deviates from the known Fe protein tertiary structure (NifH1 homodimer). A second likely function can than be proposed for NifH2, that is NifH2 may act as a regulatory protein in nitrogen-fixing cells of *C. pasteurianum*. This hypothesis cannot be supported with the available experimental data at the moment. Because both proteins travel to the same distance in acrylamide gels, it is not possible to detect their relative amount with respect to each other. Examination of Western blots indicates the presence of both proteins throughout growth. However, in Northern blots there are two time points where *nifH2* expression continues when there is no detectable *nifH1* expression after ammonia addition. Based on the results presented here and the Northern data presented elsewhere [18], it is likely that in *C. pasteurianum*, nitrogen-fixing activity is regulated with the relative amounts of NifH1 and NifH2 proteins. When the amount NifH2 elevates, it causes an increase in the number of inactive NifH1–NifH2 complexes.

In vivo and in vitro nitrogen-fixing activities before and after ammonium acetate addition show apparent differences in regulation of nitrogen-fixing activities between *C. pasteurianum* and *C. beijerinckii* [16]. After the addition of ammonium acetate, the level of in vivo nitrogenase activity stays constant in *C. pasteurianum*, whereas in *C. beijerinckii* it drops sharply. However, when growth was considered, in vivo nitrogen-fixing activity (unit/ml of culture·optical density) drops significantly in *C. pasteurianum* after ammonium acetate addition. The growth-related decrease in nitrogen-fixing activity was thought to be caused by dilution of enzyme activity due to growth because the newly generated cells did not synthesize new NifH1 protein and maintained the previously synthesized nitrogenase [9]. With the notion of the presence of a NifH1–NifH2 dimer, we may have to revisit the regulation of nitrogen fixation in *C. pasteurianum*.

Acknowledgements

The author wishes to thank Dr. Jiann-Shin Chen for introducing the author to the field of nitrogen fixation. The author also wishes to thank Dr. Ali Sazci for his thoughtful comments during preparation of the manuscript.

Appendix A. Supplementary data

Supplementary data associated with this article can be found, in the online version, at 10.1016/j.jmgm.2006.01.006.

References

[1] M. Ribbe, D. Gadkari, O. Meyers, N_2 fixation by *Streptomyces thermoautotrophicus* involves a molybdenum-dinitrogenase and a manganase-superoxide oxidoreductase that couple N_2 reduction to the oxidation of superoxide produced from O_2 by a molybdenum-CO dehydrogenase, J. Biol. Chem. 272 (1997) 26627–26633.
[2] P.E. Bishop, R. Premarkur, Alternative nitrogen fixation systems, in: G. Stacey, R.H. Burris, H.J. Evans (Eds.), Biological Nitrogen Fixation, Chapman & Hall, New York, London, 1992, pp. 736–762.
[3] J.D. Kim, D.C. Rees, X-ray crystal structure of the nitrogenase molybdenum-iron protein from *Clostridium pasteurianum* at 3.0-Å resolution, Biochemistry 32 (1993) 7104–7115.
[4] M.M. Georgiadis, H. Komiya, P. Chakrabarti, D. Wooo, J.J. Kornuc, D.C. Rees, Crystallographic structure of the nitrogenase iron protein from *Azotobacter vinelandii*, Science 257 (1992) 1653–1658.
[5] R.H. Burris, Nitrogenases, J. Biol. Chem. 266 (1991) 9339–9342.
[6] R.W. Detroy, R.A. Parejko, P.W. Wilson, Complementary functioning of two components required for the reduction of N_2 from four nitrogen fixing bacteria, Science 158 (1967) 526–527.
[7] D.W. Emerich, R.H. Burris, Complementary functioning of the component proteins of nitrogenase from several bacteria, J. Bacteriol. 134 (1978) 936–943.
[8] L.E. Mortenson, Nitrogen fixation in extracts of *Clostridium pasteurianum*, in: A.S. Pietro (Ed.), Nonheme Iron Proteins: Role in Energy Conversion, The Antioch Press & Yellow Springs, Ohio, 1965 , pp. 243–259.
[9] G. Daesch, L.E. Mortenson, Effect of ammonia on the synthesis and function of the nitrogen-fixing enzyme system in *C. pasteurianum*, J. Bacteriol. 110 (1972) 103–109.
[10] G.R. Upchurch, L.E. Mortenson, In vivo energetics and control of nitrogen fixation: changes in the adenylate charge and adenosine 5′-diphosphate/adenosine 5′-triphosphateratio of cells during growth on dinitrogen versus growth on ammonia, J. Bacteriol. 143 (1980) 274–284.
[11] S.-Z. Wang, J.-S. Chen, J.L. Johnson, The presence of five *nifH*-like sequences in *C. pasteurianum*: sequence divergence and transcriptional properties, Nucl. Acids Res. 16 (1988) 439–453.
[12] J.T. Bolin, N. Campobasso, S.W. Muchmore, W. Minor, T.V. Morgan, L.E. Mortenson, The crystal structure of the nitrogenase MoFe protein from *Clostridium pasteurianum*, in: Palacios, et al. (Eds.), New Horizons in

Nitrogen Fixation, Kluwer Academic Publishers, Netherlands, 1993, pp. 89–94.
[13] J.-S. Chen, S.-Z. Wang, J.L. Johnson, Nitrogen fixation genes of *Clostridium pasteurianum*, in: Gresshoff, Roth, Stacey, Newton (Eds.), Nitrogen Fixation: Achievements and Objectives, Chapman & Hall, New York, London, 1990.
[14] G. Daesch, L.E. Mortenson, Sucrose catabolism in *C. pasteurianum* and its relation to N_2 fixation, J. Bacteriol. 96 (1968) 346–351.
[15] B. Seto, L.E. Mortenson, In vivo kinetics of nitrogenase formation in *Clostridium pasteurianum*, J. Bacteriol. 120 (1974) 822–830.
[16] M. Kasap, Nitrogen metabolism and solvent production in *C. beijerinckii* NRRL B593, Ph.D. Thesis, Virginia Tech. Blacksburg, VA, USA, 2002.
[17] J.-S. Chen, J.L. Johnson, Molecular biology of nitrogen fixation in the clostridia, in: D.R. Woods (Ed.), The Clostridia and Biotechnology, Butterworth–Heinemann, Boston, USA, 1993, pp. 371–392.
[18] M. Kasap, J.S. Chen, *Clostridium pasteurianum* W5 synthesizes two NifH-related polypeptides under nitrogen-fixing conditions, Microbiology 151 (2005) 2353–2362.
[19] J.L. Schlessman, D. Woo, L. Joshua-Tor, J.B. Howard, D.C. Rees, Conformational variability in structures of the nitrogenase iron proteins from *Azotobacter vinelandii* and *Clostridium pasteurianum*, J. Mol. Biol. 280 (1998) 669–685.
[20] H.B. Uchoa, G.E. Jorge, N.J. Freitas Da Silveira, J.C. Camera Jr., F. Canduri, W.F. De Azevedo Jr., Parmodel: a web server for automated comparative modelling of proteins, Biochem. Biophys. Res. Commun. 325 (2004) 1481–1486.
[21] J.D. Thompson, D.G. Higgins, T.J. Gibson, CLUSTAL W: improving the sensitivity of progressive multiple sequence alignment through sequence weighting, position-specific gap penalties and weight matrix choice, Nucl. Acids Res. 22 (1994) 4673–4680.
[22] P.Y. Muller, E. Studer, A.R. Miserez, Molecular biocomputing suite: a word processor add-in for the analysis and manipulation of nucleic acid and protein sequence data, Biotechniques 6 (2001) 1310–1313.
[23] S.R. Comeau, D.W. Gatchell, S. Vajda, C.J. Camacho, ClusPro: a fully automated algorithm for protein–protein docking, Nucl. Acids Res. 32 (Web Server issue) (2004) W96–W99.
[24] S.R. Comeau, D.W. Gatchell, S. Vajda, C.J. Camacho, ClusPro: an automated docking and discrimination method for the prediction of protein complexes, Bioinformatics 20 (2004) 45–50.
[25] D.J. Jacobs, A.J. Rader, M.F. Thorpe, L.A. Kuhn, Protein flexibility predictions using graph theory, Proteins 44 (2001) 150–165.
[26] C. Chothia, A.M. Lesk, The relation between the divergence of sequence and structure in proteins, EMBO J. 4 (1986) 823–826.
[27] Y. Zhang, J. Skolnick, Scoring function for automated assessment of protein structure template quality, Proteins 57 (2004) 702–710.
[28] S.B. Jang, M.S. Jeong, L.C. Seefeldt, J.W. Peters, Structural and biochemical implications of single amino acid substitutions in the nucleotide-dependent switch regions of the nitrogenase Fe protein from *Azotobacter vinelandii*, J. Biol. Inorg. Chem. 8 (2004) 1028–1033.
[29] W.N. Lanzilotta, K. Fisher, L.C. Seefeldt, Evidence for electron transfer-dependent formation of a nitrogenase iron protein-molybdenum-iron protein tight complex. The role of aspartate 39, J. Biol. Chem. 7 (1997) 4157–4165.
[30] M.G. Duyvis, H. Wassink, H. Haaker, Pre-steady-state kinetics of nitrogenase from *Azotobacter vinelandii*. Evidence for an ATP-induced conformational change of the nitrogenase complex as part of the reaction mechanism, J. Biol. Chem. 47 (1996) 29632–29636.
[31] K.A. Renner, J.B. Howard, Aluminum fluoride inhibition of nitrogenase: stabilization of a nucleotide Fe-protein MoFe-protein complex, Biochemistry 17 (1996) 5353–5358.
[32] M.J. Ryle, W.N. Lanzilotta, L.C. Seefeldt, Elucidating the mechanism of nucleotide-dependent changes in the redox potential of the [4Fe–4S] cluster in nitrogenase iron protein: the role of phenylalanine 135, Biochemistry 29 (1996) 9424–9434.
[33] D. Wolle, D.R. Dean, J.B. Howard, Nucleotide-iron-sulfur cluster signal transduction in the nitrogenase iron-protein: the role of Asp125, Science 258 (1992) 992–995.
[34] J.E. Walker, M. Saraste, M.J. Runswick, N.J. Gay, Distantly related sequences in the alpha- and beta-subunits of ATP synthase, myosin, kinases and other ATP-requiring enzymes and a common nucleotide binding fold, EMBO J. 1 (1982) 945–951.
[35] J.W. Peters, K. Fisher, D.R. Dean, Identification of a nitrogenase protein–protein interaction site defined by residues 59 through 67 within the *Azotobacter vinelandii* Fe protein, J. Biol. Chem. 269 (1994) 28076–28083.
[36] F. Norel, C. Elmerich, Nucleotide sequence and functional analysis of the two *nifH* copies of *Rhizobium* ORS571, J. Gen. Microbiol. 133 (1987) 1563–1576.